

Wave function collapse in a mesoscopic deviceG. B. Lesovik,¹ A. V. Lebedev,¹ and G. Blatter²¹*L.D. Landau Institute for Theoretical Physics RAS, 117940 Moscow, Russia*²*Theoretische Physik, ETH-Hönggerberg, CH-8093 Zürich, Switzerland*

(Received 3 December 2004; published 15 March 2005)

We determine the nonlocal in time and space current-current cross correlator $\langle \hat{I}(x_1, t_1) \hat{I}(x_2, t_2) \rangle$ in a mesoscopic conductor with a scattering center at the origin. Its excess part appearing at finite voltage exhibits a unique dependence on the retarded variable $t_1 - t_2 - (|x_1| - |x_2|)/v_F$, with v_F the Fermi velocity. The nonmonotonic dependence of the retardation on x_1 and its absence at the symmetric position $x_1 = -x_2$ is a signature of an instantaneous wave function collapse, which thus becomes amenable to observation in a mesoscopic solid state device.

DOI: 10.1103/PhysRevB.71.125313

PACS number(s): 72.70.+m, 03.65.Ud

The recent years have seen a confluence of interests in quantum optics and condensed matter physics. This trend is particularly apparent in the field of quantum information science,¹ where quantum optical as well as mesoscopic nanoscale devices are being designed and implemented as potential hardware components for quantum computing. In addition to this technological aspect, fundamental questions traditionally investigated in quantum optical setups² are now being implemented in mesoscopic structures. Examples are the recent proposals for solid state entanglers³ and their potential use in testing Bell inequalities^{4,5} or the fermionic implementation⁶ of Hanbury-Brown-Twiss-type experiments testing for particle correlations induced by their statistical properties. Another fundamental issue is the measurement process and the associated collapse of the wave function. The latter has lately been discussed in the context of quantum measurement of quantum bits⁷⁻⁹ with the main focus on issues related to the backaction dephasing of the qubit and the acquisition of information by the detector. In the present paper, we concentrate on the wave function collapse itself and demonstrate how it can be identified and analyzed in a measurement of current cross-correlators in a mesoscopic device.

In the orthodox interpretation of quantum mechanics, the wave packet reduction is introduced as an independent postulate within the context of the measurement process.¹⁰ While the ordinary time evolution of a quantum system follows the dynamics described by the Schrödinger equation, the measurement process involves an instantaneous projection onto the pointer basis of the measurement device. Attempts to bind the wave function collapse into the conventional frame of unitary time evolution have been made, particularly in model systems describing a quantum degree of freedom coupled to a reservoir,¹¹ but with limited success so far. The experiment suggested and analyzed below will be suitable to separate an instantaneous collapse from one carrying its own dynamics through the measurement of retardation effects.

According to usual expectations, the detection of an individual particle induces a wave function collapse, however, no useful quantitative information on the collapse itself can

be extracted from such an isolated measurement. On the other hand, the wave packet reduction appears naturally in von Neumann's prescription of repeated measurements,¹⁰ motivating its experimental observation through *repeated* detection. In today's context this is realized in the measurement of correlators, e.g., the current-current correlators (noise) $\langle \hat{I}(t) \hat{I}(0) \rangle$ in a mesoscopic device. In such an experiment, the second measurement tests the change in state induced by the first measurement and hence carries the signature of the wave function collapse.

In our theoretical analysis below we stay within the framework set by the orthodox interpretation of quantum mechanics. We determine the current cross correlator within the second quantized formalism which treats the wave function collapse as an instantaneous and nonlocal process. Accordingly, our result carries the signature of an instantaneous collapse as expressed through a vanishing delay time between the appearance of particles (electrons) in one place and the vanishing of their quantum-alternative partners (appearance of holes) in the other place. On the other hand, one expects that a collapse involving its own dynamics, e.g., the unitary Schrödinger evolution, naturally leads to a finite delay which will show up in the noise experiment. Hence the proposed experiment provides quantitative information on the properties of the wave function collapse in a mesoscopic device.

To fix ideas, consider a particle wave incident from a source lead s and split with amplitudes t_{su} and t_{sd} into the upper (u) and lower (d) arms of a fork device, see Fig. 1(a). We emphasize that it is the unitary evolution dictated by wave mechanics which determines the propagation of particles into the two arms. For the time being, we ignore the possibility that the splitter projects the particles and distributes them into the two arms via a classical random process, i.e., we assume that there is no object in the splitter associated with a local hidden variable. This assumption has to be checked in the experiment and we will return back to this point later.

Hence before any measurement, the particles propagate in terms of waves and are delocalized between the two arms. A measurement of the current in one of the arms, say u ,

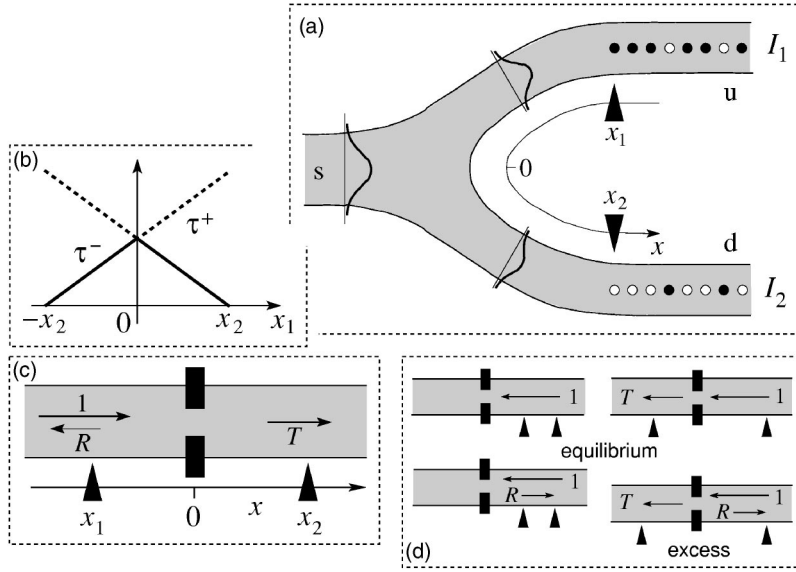


FIG. 1. (a) A splitter directs an incident wave into arms (' u ') and (' d ') with amplitudes t_{su} and t_{sd} . After measurement in u (at $t_1=t$ and $x_1 < 0$) the wave is projected resulting in a specific sequence of particles. The simultaneous measurement in arm d (at $t_2=t^+$ and $x_2=-x_1 > 0$) will detect the conjugate sequence. Shifting the measurement point in u to smaller values x_1 produces a delay $\tau^- = (|x_1| - x_2)/v_F$ in the excess noise with the symmetric dependence shown in (b). The actual calculation of the current excess noise is carried out for the quantum wire with a scatterer characterized by transmission and reflection amplitudes t and r , see (c). The processes contributing to the equilibrium and excess noise are sketched in (d).

projects the wave function and the subsequent evolution is in terms of particle streams, see Fig. 1(a). Note that we only need one measurement to project the waves to particle streams in *both* arms. However, in order to detect the (instantaneous) collapse of the wave function, we have to perform two measurements in the two arms allowing us to observe the coincidence between a particle missing in one arm and the additional particle propagating in the other arm. Such an experiment can be realized efficiently if detectors are used which react on the presence of particles in one arm and holes in the other arm. The observation of a perfect coincidence between the appearance of particles and their partner holes then is a demonstration of the instantaneous reduction of the wave function in this setup.

The information that can be extracted from the noise experiment depends crucially on its time resolution. For example, one may deliberately separate (in time) the stream of coincident events, i.e., particles and holes in d and u , by choosing an asymmetric splitter with a small transmission $T_{sd} = |t_{sd}|^2$ into one of the arms; this type of splitter has been introduced by Beenakker *et al.*⁵ in a recent proposal for the measurement of the degree of entanglement in a many body wave function. A detector with limited temporal and/or spatial resolution then is still capable of detecting individual events and thus can serve in this type of coincidence experiment; however, the limited resolution restricts the analysis of the wave function collapse and its intrinsic dynamics. On the other hand, if detectors with high resolution are used in the measurement of cross-correlators (of either current or density) a finite frequency/short time measurement can trace the signature of the wave function collapse for any value of the transmission $|t_{su}|^2$. Furthermore, a high resolution provides quantitative details on the collapse itself; in particular, it allows us to determine accurately the delay time involved in the collapse and hence an instantaneous collapse can be distinguished from a dynamical one. Typical parameters used in mesoscopic setups involve time scales of order GHz and length scales of order micrometers — one then easily checks that a dynamical collapse involving the Fermi velocity and beyond can be resolved, while a dynamical collapse involv-

ing a (super)luminal velocity is beyond the attainable resolution.

The above idea for a direct measurement of the wave function collapse can be implemented with different types of mesoscopic experiments: (a) a beam splitter in a fork geometry can be realized with the help of electrostatic gates structuring a two-dimensional electron gas as done in Ref. 6, (b) a nearly ideal splitter can be realized in a quantum Hall setup with a split gate,⁶ and (c) use can be made of a simple quantum wire with a localized scatterer where the two arms correspond to the backward and forward scattering channels, see Fig. 1(c). First, we concentrate on the last example,¹² the quantum wire, and determine the irreducible current-current cross-correlator

$$C_{x_1, x_2}(t_1 - t_2) \equiv \langle \hat{I}(x_1, t_1) \hat{I}(x_2, t_2) \rangle, \quad (1)$$

with the signal measured once on the same side of the scatterer ($x_1, x_2 > 0$) and subsequently on opposite sides ($x_1, x_2 < 0$). In the coherent conductor studied here, the excess noise $C_{x_1, x_2}^{\text{ex}}(\tau; V) \equiv C_{x_1, x_2}(\tau; V) - C_{x_1, x_2}(\tau; V=0)$ is entirely due to the quantum shot noise; the latter has been intensely studied during the past years.¹³ Most of these studies have concentrated on the low-frequency limit, identifying quasi-particle charges¹⁴ or antibunching of fermions,⁶ to name two well-known examples. While the partitioning of the particle beam due to the reduction of wave packets was clearly identified as the source of shot noise¹³ this aspect has never been analyzed in detail. The most interesting result is found for the measurement involving current fluctuations on opposite sides of the barrier: we find that the excess noise $C_{x_1, x_2}^{\text{ex}}(\tau)$ depends on a spatially retarded variable with the particular form $\tau - \tau^-$ where $\tau^- = (|x_1| - |x_2|)/v_F$, see Fig. 1(b). This should be contrasted with the ballistic retardation appearing in the equilibrium noise $C_{x_1, x_2}^{\text{eq}}(\tau; V=0)$ and exhibiting the causally retarded dependence $\tau - \tau^+$ with $\tau^+ = (|x_1| + |x_2|)/v_F$ involving the ratio of the traveling distance and the Fermi velocity. This latter type of retardation has to be expected due to the relation between the equilibrium correlator and the

(causally retarded) linear response function enforced by the fluctuation-dissipation theorem. On the contrary, the particular dependence on $\tau - \tau^-$ appearing in C^{ex} identifies the presence of instantaneous correlations between spatially separated events, which we interpret as arising from the instantaneous collapse of the wave function.

We now turn to the derivation of the above results and determine the excess noise in the current-current cross-correlator. We concentrate on the geometry sketched in Fig. 1(c) and define the field operators (for one spin component; $v_\epsilon = \sqrt{2m\epsilon}$)

$$\hat{\Psi}|_{x < 0} = \int \frac{d\epsilon}{\sqrt{hv_\epsilon}} [(e^{ikx} + r_\epsilon e^{-ikx}) \hat{a}_\epsilon + t_\epsilon e^{-ikx} \hat{b}_\epsilon] e^{-i\epsilon t/\hbar},$$

$$\hat{\Psi}|_{x > 0} = \int \frac{d\epsilon}{\sqrt{hv_\epsilon}} [t_\epsilon e^{ikx} \hat{a}_\epsilon + (e^{-ikx} + r'_\epsilon e^{ikx}) \hat{b}_\epsilon] e^{-i\epsilon t/\hbar}$$

with \hat{a}_ϵ (\hat{b}_ϵ) the electronic annihilation operators for the left (right) reservoir and t , r , r' the usual scattering amplitudes. Substituting these expressions into the current operator $\hat{I}(x, t) = (ie\hbar/2m) [\partial_x \hat{\Psi}^+(x) \hat{\Psi}(x) - \hat{\Psi}^+(x) \partial_x \hat{\Psi}(x)]$ and using the standard scattering theory of noise,^{13,15,16} we obtain the expression for the current-current cross correlator (1). We split the result into an equilibrium part $C_{x_1 x_2}^{\text{eq}}(\tau)$ and an excess part $C_{x_1 x_2}^{\text{ex}}(\tau)$ with $\tau = t_1 - t_2$; correlators evaluated at the same side of the scatterer are denoted by \bar{C} , those on opposite sides by C . Assuming $|\epsilon' - \epsilon| \sim eV \ll \epsilon_F$, with V the applied voltage and ϵ_F the Fermi energy, we drop terms¹⁶ small in the parameter $|\epsilon' - \epsilon|/\epsilon_F$ and find the result for $x_1 x_2 < 0$ [the Fermi occupation numbers $n_L(\epsilon)$ and $n_R(\epsilon)$ denote the filling of the attached reservoirs],

$$\begin{aligned} C_{x_1 x_2}^{\text{eq}}(\tau) &= \frac{2e^2}{h^2} \int d\epsilon d\epsilon' e^{i(\epsilon' - \epsilon)\tau/\hbar} [t_\epsilon t_{\epsilon'}^* e^{i(\epsilon' - \epsilon)\tau^+/\hbar} n_L(\epsilon') \\ &\quad \times [1 - n_L(\epsilon)] + t_\epsilon^* t_{\epsilon'} e^{-i(\epsilon' - \epsilon)\tau^+/\hbar} n_R(\epsilon') [1 - n_R(\epsilon)]], \end{aligned} \quad (2)$$

while the corresponding result evaluated on the same side of the scatterer ($x_1 x_2 > 0$) takes the form

$$\begin{aligned} \bar{C}_{x_1 x_2}^{\text{eq}}(\tau) &= \frac{2e^2}{h^2} \int d\epsilon d\epsilon' e^{i(\epsilon' - \epsilon)\tau/\hbar} [T_{\epsilon'} e^{-i(\epsilon' - \epsilon)\tau^-/\hbar} n_L(\epsilon') \\ &\quad \times [1 - n_L(\epsilon)] + (e^{i(\epsilon' - \epsilon)\tau^-/\hbar} + R_{\epsilon'} e^{-i(\epsilon' - \epsilon)\tau^-/\hbar}) n_R(\epsilon') \\ &\quad \times [1 - n_R(\epsilon)] - (r'_\epsilon t_{\epsilon'}^* e^{i(\epsilon' - \epsilon)\tau^+/\hbar} + \text{c.c.}) n_R(\epsilon') \\ &\quad \times [1 - n_R(\epsilon)]]. \end{aligned} \quad (3)$$

The time dependence appearing in Eqs. (3) and (4) involves the retardations

$$\tau^\pm = (|x_1| \pm |x_2|)/v_F \quad (4)$$

with v_F the Fermi velocity. The excess part $C_{x_1 x_2}^{\text{ex}}(\tau)$ is given by the expressions

$$\begin{aligned} C_{x_1 x_2}^{\text{ex}}(\tau) &= \frac{2e^2}{h^2} \int d\epsilon d\epsilon' e^{i(\epsilon' - \epsilon)(\tau - \tau^-)/\hbar} t_\epsilon^* t_{\epsilon'} r_{\epsilon'}^* r_\epsilon [n_L(\epsilon') \\ &\quad - n_R(\epsilon')] [n_L(\epsilon) - n_R(\epsilon)], \end{aligned} \quad (5)$$

$$\begin{aligned} \bar{C}_{x_1 x_2}^{\text{ex}}(\tau) &= \frac{2e^2}{h^2} \int d\epsilon d\epsilon' e^{i(\epsilon' - \epsilon)(\tau - \tau^-)/\hbar} [T_{\epsilon'} R_\epsilon n_L(\epsilon') \\ &\quad - R_{\epsilon'} T_\epsilon n_R(\epsilon')] [n_L(\epsilon) - n_R(\epsilon)], \end{aligned} \quad (6)$$

with the unique retardation τ^- . In the following, we drop the energy dependencies of the scattering amplitudes, allowing us to perform the integration over energies, and we find the simplified expressions (we denote the temperature by θ and assume $k_B = 1$)

$$C_{x_1 x_2}^{\text{eq}}(\tau, \theta) = - \frac{2e^2 T}{h^2} [\alpha(\tau + \tau^+, \theta) + \alpha(\tau - \tau^+, \theta)],$$

$$\begin{aligned} \bar{C}_{x_1 x_2}^{\text{eq}}(\tau, \theta) &= - \frac{2e^2}{h^2} \alpha(\tau + \tau^-, \theta) + \alpha(\tau - \tau^-, \theta) - R[\alpha(\tau + \tau^+, \theta) \\ &\quad + \alpha(\tau - \tau^+, \theta)], \end{aligned}$$

$$C_{x_1 x_2}^{\text{ex}}(\tau, \theta) = \frac{8e^2 TR}{h^2} \sin^2 \left[\frac{eV(\tau - \tau^-)}{2\hbar} \right] \alpha(\tau - \tau^-, \theta), \quad (7)$$

with the temperature dependence given by the expression $\alpha(\tau, \theta) = \pi^2 \theta^2 / \sinh^2[\pi \theta \tau / \hbar]$; in the zero-temperature limit this reduces to $\alpha(\tau, 0) = \hbar^2 / \tau^2$. The singularity at $\tau \rightarrow 0$ is cutoff for $\tau < \hbar / \epsilon_F$ and the equilibrium correlator changes sign as individual fermions extending over the Fermi wavelength λ_F are probed; proper calculation of this feature requires us to account for the finite Fermi energy and bandwidth of the electron system. Quite remarkably, the excess noise is given by a unique expression and involves only the retardation τ^- . The above results apply for the quantum wire, see Fig. 1(b). The result (7) for the excess noise is easily rewritten for the fork geometry in Fig. 1(a) by replacing the product of transmission and reflection probabilities TR by the product $-T_{su} T_{sd}$, with T_{su} and T_{sd} the transmission probabilities from the source lead s into the upper (u) and lower (d) leads. The sign change is due to the current reversal as the reflected beam in the quantum wire is replaced by a second forward directed beam in the fork geometry.

Let us analyze the results (7) in more detail. Consider first the equilibrium noise. The sign of the correlator follows from the fact that a, say positive, current fluctuation is followed by a compensating and hence negative excursion. The terms $\propto 1$ and $\propto R$ appearing in \bar{C}^{eq} derive from correlations in the incident flow and between the incident and reflected flow, while C^{eq} measures correlations between the incident and transmitted waves and hence involves the transmission coefficient T , see the diagrams in Fig. 1(d). The signs are as expected from the above argument (note the sign change in the term $\propto R$ due to the current reversal) and all retardations are causal involving the geometric distance between particle detection. The symmetry $\tau \leftrightarrow -\tau$ is due to the equivalence of the two reservoirs injecting particles symmetrically under equilibrium conditions.

The excess noise measures correlations between the transmitted and reflected particles, see Fig. 1(d). Its retardation and sign are those expected assuming an instantaneous collapse of the wave function. That is, projecting the wave by the detection of an electron at x_1 implies the instantaneous appearance of a hole at x_2 traveling in the opposite direction, thus resulting in a positive sign of C^{ex} (note the change in sign when going from the point contact to the fork geometry). Furthermore, the vanishing of the relaxation time τ right at the symmetric location $x_1 = -x_2$ is the hallmark of the instantaneous collapse of the wave function. On the other hand, the observation of a nonzero time delay (at the symmetric location $x_1 = -x_2$) would indicate the presence of a nontrivial dynamical element in the process of wave function collapse beyond the framework of the orthodox theory with its projection postulate. Hence measuring the excess noise in an experiment and comparing to our result (7) allows us to confirm or refute the instantaneous and nonlocal nature of the wave function collapse. Finally, the oscillations appearing in the excess noise are a consequence of the sharp Fermi surfaces, their scale $\delta\tau \sim h/eV$ being determined by the voltage shift eV between the reservoirs; a temperature $\theta > eV$ smears this sharp shift and the tails with their oscillations vanish exponentially $\propto \exp(-2\pi\tau\theta/\hbar)$.

Above, we have emphasized the quantum nature of wave propagation in our determination of the excess noise. One may ask about the outcome of this experiment within a classical model of electronic transport, where the splitter randomly distributes the (ordered stream of) particles among the two arms of the fork [see Fig. 1(a)] or, in our geometry, in the forward and backward directions [see Fig. 1(c)]. Indeed, particles sent into the forward direction then are correlated with missing particles (holes) in the backward flow and the correlator has the same sign and retardation as in the quantum case. Note, that the particular retardation given by τ^- has a different origin in the classical and in the quantum case: in the classical situation where particle-hole pairs are locally generated at the splitter, the delay derives from the difference in the travelling times of the particle and the hole, while in the quantum case, the particle-hole pairs appear due to the nonlocal process of instantaneous projection.

A meaningful experiment has to distinguish between the classical and the quantum-mechanical scenario producing the measured results. In order to show that quantum mechanics is at work one has to confirm the wave propagation in the device prior to measuring the current cross correlator. This can be achieved through the observation of a coherence phenomenon and we discuss two specific setups in the following.

(i) Inserting a second barrier, the observation of resonant transmission through the interferometer formed by the double barrier system confirms the wave propagation in the device. An implementation using electrostatic gates modulating a 2DEG allows us to manipulate the second barrier without significant perturbation of the remaining sample.

(ii) Following ideas developed within the context of the famous double slit (Gedanken) experiment, we propose the specific setup sketched in Fig. 2 which tests the particle-wave duality during the experiment. The incident particle beam s is split into an upper (u) and lower (d) arm (fork

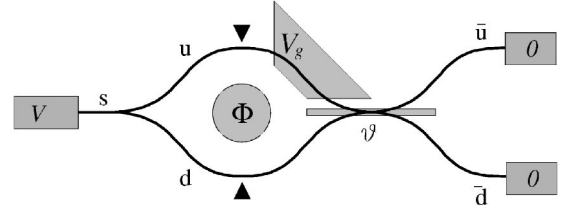


FIG. 2. Experimental setup testing the wave propagation of electrons before projecting the wave function in the noise measurement. In a first step, the phase difference $\delta\varphi = \varphi_u - \varphi_d$ picked up in the propagation along the upper (u) or lower arm (d) and the mixing angle ϑ of the four-beam splitter are arranged such that no electrons propagate into the upper arm \bar{u} ; the phase $\delta\varphi$ may be manipulated through changing the flux Φ through the loop or via an electric gate potential V_g . Next, the noise correlator is measured (black triangles), projecting the electrons in the arms u and d and transforming the wave propagation into a flow of discrete particles. As a result of this projection, a finite current turns on in the upper arm \bar{u} .

geometry) and subsequently recombined and redirected into the leads \bar{u} and \bar{d} with the help of a tunable reflectionless four-beam splitter. The phase difference $\delta\varphi = \varphi_u - \varphi_d$ picked up during the propagation in the upper and lower leads can be tuned, either via a magnetic flux Φ threading the loop or via an additional gate electrode biasing (with V_g) one of the arms. The second beam splitter is characterized through its transfer matrix $M_{ud}^{u\bar{d}}$

$$\begin{pmatrix} \bar{u} \\ \bar{d} \end{pmatrix} = \underbrace{\begin{pmatrix} e^{i\phi} \cos \vartheta & -e^{i\psi} \sin \vartheta \\ e^{-i\psi} \sin \vartheta & e^{-i\phi} \cos \vartheta \end{pmatrix}}_{M_{ud}^{u\bar{d}}} \begin{pmatrix} u \\ d \end{pmatrix}, \quad (8)$$

with the angles $\vartheta \in (0, \pi/2)$, $\phi, \psi \in (0, 2\pi)$; without loss of generality we assume $\phi = \psi = 0$. The wave function behind the splitter then can be written in the form

$$\begin{aligned} \bar{\Psi}_{\bar{u}\bar{d}} = & (\cos \vartheta e^{i\varphi_u} t_{su} - \sin \vartheta e^{i\varphi_d} t_{sd}) |\bar{u}\rangle + (\sin \vartheta e^{i\varphi_u} t_{su} \\ & + \cos \vartheta e^{i\varphi_d} t_{sd}) |\bar{d}\rangle. \end{aligned} \quad (9)$$

The four-beam splitter shall be tuned such that all electrons propagate to only one of the output leads, say the down lead \bar{d} , implying the condition $\tan \vartheta_0 = \sqrt{T_{su}/T_{sd}} \exp[i(\delta\varphi + \chi_{su} - \chi_{sd})]$, where we have separated the amplitudes and phases of the transmission coefficients $t_{su} = \sqrt{T_{su}} \exp(i\chi_{su})$ and similar for t_{sd} . Tuning the phase $\delta\varphi + \chi_{su} - \chi_{sd}$ to a multiple of 2π and choosing the appropriate angle

$$\tan \vartheta_0 = \sqrt{T_{su}/T_{sd}} \quad (10)$$

one may redirect the recombined waves into the down lead. Furthermore, subsequent scanning of the phase $\delta\varphi$ will produce an oscillating current in the output lead \bar{d} , analogous to the intensity oscillations observed on the detector screen in the double split experiment. The observation of current oscillations as a function of $\delta\varphi$ proves the coherent wave propagation of the electrons through the device.

After establishing the quantum nature of the electron propagation, the wave packet reduction is investigated

through a measurement of the current cross-correlator between the two arms u and d . This measurement and its concomitant wave function collapse will transform the wave propagation in the two arms into streams of particles. As a consequence of the projection through the measurement a finite current will appear in the upper lead \bar{u} . The magnitude of this current is determined with the help of the density matrix $\bar{\rho}$ behind the four-beam splitter: transforming the density matrix $\rho = T_{su}|u\rangle\langle u| + T_{sd}|d\rangle\langle d|$ describing the electron streams in the two arms u and d after the projection with the help of Eq. (8), we obtain the current $\langle \hat{I}_{\bar{u}} \rangle = 2(e^2/h)V\bar{\rho}_{mm}$ with

$$\bar{\rho}_{mm} = \langle \bar{u} | \bar{\rho} | \bar{u} \rangle = T_{su} \cos^2 \vartheta_0 + T_{sd} \sin^2 \vartheta_0 = 2 \frac{T_{su}T_{sd}}{T_{su} + T_{sd}}, \quad (11)$$

where we have made use of Eq. (10) in the last equation. For a reflectionless splitter we have $T_{su} + T_{sd} = 1$ and the final result for the current appearing in the lead \bar{u} after projection takes the form

$$\langle \hat{I}_{\bar{u}} \rangle = 4(e^2/h)VT_{su}T_{sd}. \quad (12)$$

The maximum difference between the currents with and without projection is obtained for the symmetric splitter with $T_{su} = T_{sd} = 1/2$.

The above two-step procedure confirming the wave propagation of the electrons before the measurement of the current cross correlator excludes a classical interpretation of the features showing up in the noise correlator; analyzing the time delay τ^- in the excess noise then provides the sought for information on the wave function collapse. In particular, the instantaneous collapse should manifest itself through a zero time delay if a symmetric setup with $x_1 = -x_2$ is chosen; on the other hand, one expects that a collapse within the frame of unitary time evolution produces a finite delay which the present experiment is able to detect, provided the time resolution of the noise measurement is adequate.

The test for the instantaneous wave function collapse discussed here is related to the nonlocal properties of quantum mechanics. The standard test demonstrating the nonlocal nature of quantum mechanics is due to Bell.¹⁷ Bell inequality tests produce different outcomes within a classical framework (based on local hidden variables) and within a quantum-mechanical description. On the other hand, the measurement of correlators, while producing interesting results on fundamental issues of quantum mechanics, too, cannot separate between the quantum mechanical and the classical predictions. A prominent example is the measurement of strangeness correlations in the $K^0\bar{K}^0$ system: The decay of the kaons prevents one from carrying out Bell inequality tests. Still, the observation of oscillations in the strangeness correlation provides information on the entanglement in the kaon wave function.¹⁸ Nevertheless, this type of oscillations can be generated within the framework of a hidden variable theory, too. In the present case, the measurement of the noise correlator provides information on the wave function collapse, in particular, its dynamics. Again, the experiment itself cannot separate between quantum mechanical and classical

predictions. In fact, a local hidden variable at the splitter could emulate the shape of the time resolved correlator including even the oscillations on the time scale $\tau_V = \hbar/eV$. One then may assume one of the following two view points. (a) Accepting the applicability of quantum mechanics one only needs to rule out the presence of dephasing in the device; the absence of dephasing is most simply confirmed through the observation of the time oscillation $\propto \sin^2(eV \delta\tau/2\hbar)$ in the correlator itself. (b) Those critical about the validity of quantum mechanics first have to confirm the wave dynamics in the device; the experiments (i) and (ii) described above are designed to achieve this goal.

The current correlator is not directly measured in an experiment; e.g., an old-fashioned Ampère meter determines the angular excursion of the pick-up loop. One then has to relate the correlator of this classical meter variable to the correlator of the quantum system.¹⁹ For a linear detector, one expects that the measured classical correlator can be constructed from the quantum correlator through a linear connection. Conventional wisdom tells that it is the symmetric correlator that appears in an actual measurement.²⁰ Indeed, a recent analysis carried out for an Ampère meter measuring local current-correlations shows that the main term in the response is determined by the symmetrized correlator $[C(\tau) + C(-\tau)]/2$;¹⁹ however, additional small corrections appear involving the antisymmetrized correlator, too. The generalization to measurements at spatially separated locations relates the measured correlator to the fully symmetrized expression $[C_{x_1, x_2}(\tau) + C_{x_1, x_2}(-\tau) + C_{x_2, x_1}(\tau) + C_{x_2, x_1}(-\tau)]/4$ as the main term.

Alternatively, the signature of the wave function collapse may be detected in a frequency domain experiment; the result for the spectral power $S_{x_1, x_2}^{\text{ex}}(\omega) = \int d\tau C_{x_1, x_2}^{\text{ex}}(-\tau) \exp(i\omega\tau)$ of the excess noise takes the form

$$S_{x_1, x_2}^{\text{ex}}(\omega) = \frac{2e^2TR}{h} e^{-i\omega\tau^-} \left[\frac{\hbar\omega + eV}{1 - e^{-(\hbar\omega + eV)/\theta}} + \frac{\hbar\omega - eV}{1 - e^{-(\hbar\omega - eV)/\theta}} - \frac{2\hbar\omega}{1 - e^{-\hbar\omega/\theta}} \right] \quad (13)$$

and contains the characteristic delay τ^- as a phase factor. Again, a detailed analysis is required in order to relate the experimentally measured quantity to the current excess noise. For the case of an inductive measurement with an LC circuit and coinciding positions $x_1 = x_2$ such a study has been carried out;²¹ here, it is the symmetrized power $[S_{x_1, x_2}^{\text{ex}} + S_{x_2, x_1}^{\text{ex}}]_{\Omega > 0}/2$ which can be measured via the charge fluctuations on the capacitor in an LC circuit with two pick-up loops at x_1 and x_2 .

The above analysis has been carried out within a noninteracting approximation. Accounting for the effect of Coulomb interaction one may worry that the noise signal is damped due to the smoothing produced by (longitudinal) screening; the latter involves the Fermi velocity v_F . On the other hand, the incoming electrons propagate (also with Fermi velocity) in the form of a regular sequence of wave packets separated by the single particle correlation time²² $\tau_V = \hbar/eV$, a consequence of the Fermi statistics of electrons.

The screening of the density modulation on scale $v_F\tau_V$ then involves a time scale τ_V or longer. As the time resolved noise correlator also peaks on the time scale τ_V one expects that screening modifies the shape of the noise correlator but preserves its basic form. This conclusion agrees with the observation that shot noise is usually observed with the large amplitude obtained within a noninteracting approximation. Unfortunately, only few detailed theoretical results are available on the modification of shot noise due to interaction: in a diffusive conductor the zero-frequency noise $S(0)$ is even enhanced due to Coulomb effects;²³ the analysis of a ballistic quantum point contact with a large transmission produces again an enhancement of $S(0)$, while the shot noise is weakly reduced in the tunneling limit.²⁴ Finally, weak interactions can be accounted for via an energy dependent renormalization of the scattering matrix²⁵ leading to a broadening of the electron wave packets, in agreement with the above discussion.

Dephasing due to interactions among the particles or with the environment acts differently on the electrons propagating in the two leads and causes an exponential damping of the excess correlator on the coherence length L_φ . As a consequence, the sum of distances x_1 and x_2 should be chosen smaller than L_φ . An additional requirement is a sufficient experimental time resolution: with a peak width in $C_{x_1, x_2}^{\text{ex}}(\tau)$ given by $\tau_p = \max[h/eV, 1/\nu_m]$, with ν_m the cutoff frequency in the measurement setup, only shifts $|\tau^-| > \tau_p$ can be resolved. Assuming a frequency resolution in the 10 GHz regime²⁶ the peak in $C_{x_1, x_2}^{\text{ex}}(\tau)$ can be resolved for voltages

below 0.1 meV. Given a typical value $v_F \sim 10^4$ cm/s for the Fermi velocity this corresponds to a spatial resolution $v_F/\nu_m \sim 100$ Å. The comparison with a typical mesoscopic dimension of $L \sim \mu\text{m}$ scale demonstrates that potential delays expected for a collapse with a unitary time evolution can be observed well beyond the scale of the Fermi velocity. However, the observation of a superluminal collapse would require frequencies $c/L \sim 10^{14}$ s⁻¹ in the 100 THz regime as well as large voltages of the order of volts, both well beyond the acceptable range.

To conclude, we have suggested an experiment testing for the instantaneous wave function collapse in a solid-state setup based on the time resolved measurement of current-current cross correlations at spatially separated points. This scheme allows to investigate details of the wave function collapse itself, provided a sufficiently high frequency resolution is available in the experiment. While measurements of time delays due to a unitary collapse involving super-Fermi velocities are within experimental reach, the type of mesoscopic setup described here cannot trace time delays arising from a collapse involving superluminal velocities.

We acknowledge financial support from the Swiss National Foundation (through the program MaNEP, SCOPES, and CTS-ETHZ), the Landau Scholarship of the FZ Jülich, the Russian Science Support Foundation, the Russian Ministry of Science, and the program ‘‘Quantum Macrophysics’’ of the RAS.

¹A. Steane, Rep. Prog. Phys. **61**, 117 (1998).

²See A. Aspect, Nature (London) **398**, 189 (1999), and references therein.

³G. Lesovik, Th. Martin, and G. Blatter, Eur. Phys. J. B **24**, 287 (2001); P. Recher, E. V. Sukhorukov, and D. Loss, Phys. Rev. B **63**, 165314 (2001); C. Bena, S. Vishveshwara, L. Balents, and M. P. A. Fisher, Phys. Rev. Lett. **89**, 037901 (2002).

⁴N. M. Chtchelkatchev, G. Blatter, G. B. Lesovik, and Th. Martin, Phys. Rev. B **66**, 161320 (2002); P. Samuelsson, E. V. Sukhorukov, and M. Büttiker, Phys. Rev. Lett. **91**, 157002 (2003).

⁵C. W. J. Beenakker, C. Emary, M. Kindermann, and J. L. van Velsen, Phys. Rev. Lett. **91**, 147901 (2003).

⁶M. Henry, S. Oberholzer, C. Strunk, T. Heinzl, K. Ensslin, M. Holland, and C. Schonenberger, Science **284**, 296 (1999); W. D. Oliver, J. Kim, R. C. Liu, and Y. Yamamoto, *ibid.* **284**, 299 (1999).

⁷Y. Makhlin, G. Schön, and A. Shnirman, Rev. Mod. Phys. **73**, 357 (2001).

⁸A. N. Korotkov, Phys. Rev. B **63**, 115403 (2001).

⁹D. V. Averin, Phys. Rev. Lett. **88**, 207901 (2002).

¹⁰J. von Neumann, *Mathematical Foundations of Quantum Mechanics* (Princeton University Press, Princeton, 1955).

¹¹A. J. Leggett, S. Chakravarty, A. T. Dorsey, M. P. A. Fisher, A. Garg, and W. Zwerger, Rev. Mod. Phys. **59**, 1 (1987); W. H. Zurek, *ibid.* **75**, 715 (2003).

¹²After proper redefinition of flow directions the main result (7) for the excess noise in the wire also applies to the fork with an ideal splitter, see later.

¹³Y. M. Blanter and M. Büttiker, Phys. Rep. **336**, 1 (2000); *Noise in Mesoscopic Physics*, Vol. 97 of NATO Science Series, edited by Y. Nazarov (Kluwer, Delft, 2003).

¹⁴V. A. Khlus, Sov. Phys. JETP **66**, 1243 (1987); C. L. Kane and M. P. A. Fisher, Phys. Rev. Lett. **72**, 724 (1994); J. Torrès, T. Martin, and G. B. Lesovik, Phys. Rev. B **63**, 134517 (2001), and references therein; L. Saminadayar and D. C. Glatli, Phys. Rev. Lett. **79**, 2526 (1997); R. dePicciotto, M. Reznikov, M. Heiblum, V. Umansky, G. Bunin, and D. Mahalu, Nature (London) **389**, 162 (1997); A. A. Kozhevnikov, R. J. Schoelkopf, and D. E. Prober, Phys. Rev. Lett. **84**, 3398 (2000); X. Jehl, M. Sanquer, R. Calemczuk, and D. Mailly, Nature (London) **405**, 50 (2000).

¹⁵G. B. Lesovik, JETP Lett. **49**, 592 (1989).

¹⁶G. B. Lesovik, JETP Lett. **70**, 208 (1999).

¹⁷J. S. Bell, Physics (Long Island City, N.Y.) **1**, 195 (1965).

¹⁸A. Apostolakis *et al.* Phys. Lett. B **422**, 339 (1998); N. Gisin and A. Go, Am. J. Phys. **69**, 264 (2001).

¹⁹G. B. Lesovik, Phys. Usp. **41**, 145 (1998) (available from www.ufn.ru).

²⁰L. D. Landau and E. M. Lifshitz, *Statistical Physics* (Pergamon Press, London, 1958), Vol. 5 Sec. 117.

²¹G. B. Lesovik and R. Loosen, JETP Lett. **65**, 295 (1997); U.

- Gavish, Y. Levinson, and Y. Imry, Phys. Rev. B **62**, R10637 (2000).
- ²²L. S. Levitov, H. Lee, and G. B Lesovik, J. Math. Phys. **37**, 4845 (1996).
- ²³K. E. Nagaev, Phys. Rev. B **52**, 4740 (1995).
- ²⁴A. V. Galaktionov D. S. Golubev, and A. D. Zaikin, Phys. Rev. B **68**, 085317 (2003).
- ²⁵M. Kindermann and Yu. V. Nazarov, Phys. Rev. Lett. **91**, 136802 (2003).
- ²⁶R. J. Schoelkopf, P. J. Burke, A. A. Kozhevnikov, and D. E. Prober, Phys. Rev. Lett. **78**, 3370 (1997).